



Modeling the impacts of climate change on hydrological processes in the Baro–Akobo River basin, Ethiopia

Abiy Getachew Mengistu^{1,2} · Tekalegn Ayele Woldesenbet² · Yihun Taddele Dile³ · Haimanote Kebede Bayabil⁴

Received: 13 April 2022 / Accepted: 13 October 2022 / Published online: 30 November 2022

© The Author(s) under exclusive licence to Institute of Geophysics, Polish Academy of Sciences & Polish Academy of Sciences 2022

Abstract

Understanding the impacts of climate change on basin hydrology is critical for developing effective water management practices. This study was conducted to investigate climate change and its impact on the hydrological processes of the Baro–Akobo River basin in Ethiopia. Five bias-corrected regional climate models and their ensemble were developed to examine future climate changes in the 2030s (2021–2050) and 2080s (2071–2100) periods under the two Representative Concentration Pathways (RCP) 4.5 and RCP8.5 scenarios compared to a baseline (1981–2010) period. The calibrated model performed well with Nash–Sutcliffe efficiency and coefficient of determination of each 0.73 for daily and 0.89 and 0.9 for monthly simulation, respectively. Though all RCMs agree concerning the increasing direction of the 2030 and 2080s maximum and minimum temperature changes, there is inconsistency in the magnitude and direction of monthly projected rainfall changes. With the ensemble, the maximum and minimum temperatures will increase by 2.6 and 3.6 °C, respectively, and rainfall will decrease by 5% in the 2080s under RCP8.5 scenarios. The dry and wet season rainfall are expected to decrease by 19 and 3.7% under the RCP8.5 scenarios in the 2080s. Consequently, future climate change could cause a decrease in the annual surface runoff and water yield, while evapotranspiration could increase under the RCP4.5 and RCP8.5 scenarios. This study provides useful insights about potential climate change impacts on the hydrology of the basin, which could be useful to inform decision-makers in developing strategies such as water harvesting to mitigate the impact of climate change.

Keywords Climate projection · Hydrological response · SWAT · Baro–Akobo basin

Introduction

The global climate model (GCM) climate predictions provide a general view of how the earth's climate system may be affected in the future (IPCC 2007). Greenhouse gas emissions have considerably increased since the industrial

revolution and led to global warming (Van Vuuren et al. 2011). The Intergovernmental Panel on Climate Change (IPCC) found that the concentration of carbon dioxide (CO₂) in the atmosphere increased from 280 ppm in 1750 to 367 ppm in 1999 (Houghton et al. 2001). The concentration is expected to reach 463–623 ppm in 2060 and 470–1099 ppm by 2100 (Prentice et al. 2001). Increased greenhouse gas emissions are predicted to raise the average global temperature by up to 1.4–5.8 °C by the 2080s (Hoegh-Guldberg and Bruno 2010). In general, global surface temperature rise, variability of rainfall patterns, as well as changes in the predictability of this variance, are all expected in the future period (Bolch et al. 2012; Dile et al. 2013; Getachew et al. 2021; Worku et al. 2021; Liu et al. 2022). Thus, it is commendable to advance climate research using reliable information for climate impact assessment and adaptation decision-making.

Climate change scenarios can be developed using the results of global circulation models (GCMs). However, the resolution of GCMs (approximately 250 km) might be

Edited by Dr. Michael Nones (CO-EDITOR-IN-CHIEF).

✉ Abiy Getachew Mengistu
abiygetachew@aau.edu.et

- ¹ Department of Natural Resource Management, Mizan–Tepi University, Mizan-Aman, Ethiopia
- ² Ethiopian Institute of Water Resource, Addis Ababa University, Addis Ababa, Ethiopia
- ³ College of Agriculture and Life Sciences, Texas A&M University, College Station, TX, USA
- ⁴ Agricultural and Biological Engineering, Tropical Research and Education Center, Institute of Food and Agricultural Sciences, University of Florida, Homestead, FL 33031, USA

too low for basin-scale hydrological modeling. Statistical downscaling is one method of bridging this scale gap (e.g., Munawar et al. 2022), and an alternative method is dynamical downscaling, a regional climate model (RCM) employs GCM output as initial and lateral boundary conditions over a region of interest (e.g., Fowler and Kilsby 2007; Teutschbein and Seibert 2010). The higher horizontal resolution of an RCM (approximately 10–50 km) provides a better representation of topography and land-sea surface characteristics (Christensen et al. 2008). However, the RCMs are vulnerable to systematic model errors because of incorrect conceptualization, discretization, and spatial averaging within grid cells (Teutschbein and Seibert 2010, 2012). Because of this, the use of RCM simulations as a direct input of data for hydrological impact studies is challenging. As a result, using an ensemble of RCM simulations and bias correction techniques is recommended (Giorgi 2006; Déqué et al. 2007; Teutschbein and Seibert 2010; Worku et al. 2021).

Several studies were conducted in the Eastern Nile basin, particularly in the Upper Blue Nile basin (Abdo et al. 2009; Elshamy et al. 2009; Beyene et al. 2010; Setegn et al. 2011; Mengistu and Sorteberg 2012; Dile et al. 2013; Fentaw et al. 2018; Taye et al. 2018; Woldesenbet et al. 2018; Worqlul et al. 2018; Worku et al. 2021; Muleta 2021); but only limited studies were conducted in the Baro–Akobo River basin (Fentaw et al. 2018; Muleta 2021). The majority of these studies were based on statistically downscaled single GCMs that relied on the third phase of the Coupled Model Intercomparison Project (CMIP3) (e.g., Abdo et al. 2009; Worqlul et al. 2018). Some of these studies used a single GCM/RCM with single emission scenario (Soliman et al. 2009; Muleta 2021). Nevertheless, there are few studies that use bias-corrected RCM outputs and their ensemble (Elshamy et al. 2009; Worku et al. 2021) as inputs to climate impact studies. As a result, these studies have revealed mixed findings on the influence of climate on hydrological modeling. For instance, an increase in streamflow was indicated by Dile et al. (2013) and Fentaw et al. (2018) using GCM/RCM outputs in the Upper Blue Nile basin. In contrast, Elshamy et al. (2009) and Worku et al. (2021) projected a decrease in the streamflow in the Ethiopian highlands using bias-corrected GCMs and RCMs, respectively. This implies that there is no conclusive finding regarding how climate change will affect streamflow. Additionally, to the best of our knowledge, the combined use of the soil and water assessment model and the indicators of hydrological alteration for hydrological evaluation under the RCP4.5 and RCP8.5 scenarios are often missing in the aforementioned studies. Therefore, it is important to identify and describe the climate change uncertainties in the basin using a multi-climate model combined with bias correction. In addition, it is suggested to use the bias-corrected ensemble of RCM outputs for regional impact assessment.

This research was carried out in the Eastern Nile's Baro–Akobo River basin, which is known as one of the most productive areas in the country and serves as the headstream of the Eastern Nile River. Several projects related to irrigation and hydropower are ongoing under the government of Ethiopia (Tahani et al. 2013) that will pose environmental effects on the basin and downstream countries such as Sudan and Egypt. Moreover, the basin is highly vulnerable to changes in climate and extreme occurrences such as drought and flooding are projected in the future (IPCC 2014). Nonetheless, the basin has witnessed substantial climate change during the last four decades (NAPA 2007), adding to the challenges of water resource management. The majority of the population relies on rain-fed agriculture for their living, which is constantly impacted by climate change. This shows that climate change would have a considerable influence on smallholder farmers' livelihoods, necessitating thorough climate impact assessments to support climate change adaptation strategies. However, there is a limitation to integrating climate information and climate adaptation strategies to reduce climate change impacts in the basin (Conway and Schipper 2011). The increasing demand for water in the basin due to socioeconomic progress and high demand for irrigation and hydropower may cause conflict in the basin unless a comprehensive water resource management plan is developed. In addition, the impact of climate change on the different hydrological processes is poorly understood in this poorly gauged river basin. Therefore, assessing the availability of water resources in the basin in a changing climate is a prerequisite to implementing evidence-based water management options.

Thus, this study is important to provide plausible climate information generated from different bias-corrected RCMs and their ensemble rainfall and temperature outputs under different emission scenarios. It is also important to assess the impact of climate change on the hydrology of the basin in the future by considering various indicators of hydrological alteration that have been overlooked by previous studies. Such information plays a vital role in supporting the existing and planned water resources management practices in the basin. Therefore, the objectives of this study are: (1) to evaluate the variations between multiple RCMs in simulating climate over the Baro–Akobo River basin under the RCP4.5 and RCP8.5 scenarios, and (2) to evaluate the climate change impact on the basin hydrological processes implied by the ensemble results from the various RCMs of the RCP4.5 and RCP8.5 scenarios using the Soil and Water Assessment Tool (SWAT) model and the indicators of hydrological alteration.

Study area

The Baro–Akobo River basin is one of the 12 major river basins in Ethiopia (Fig. 1). It drains from the

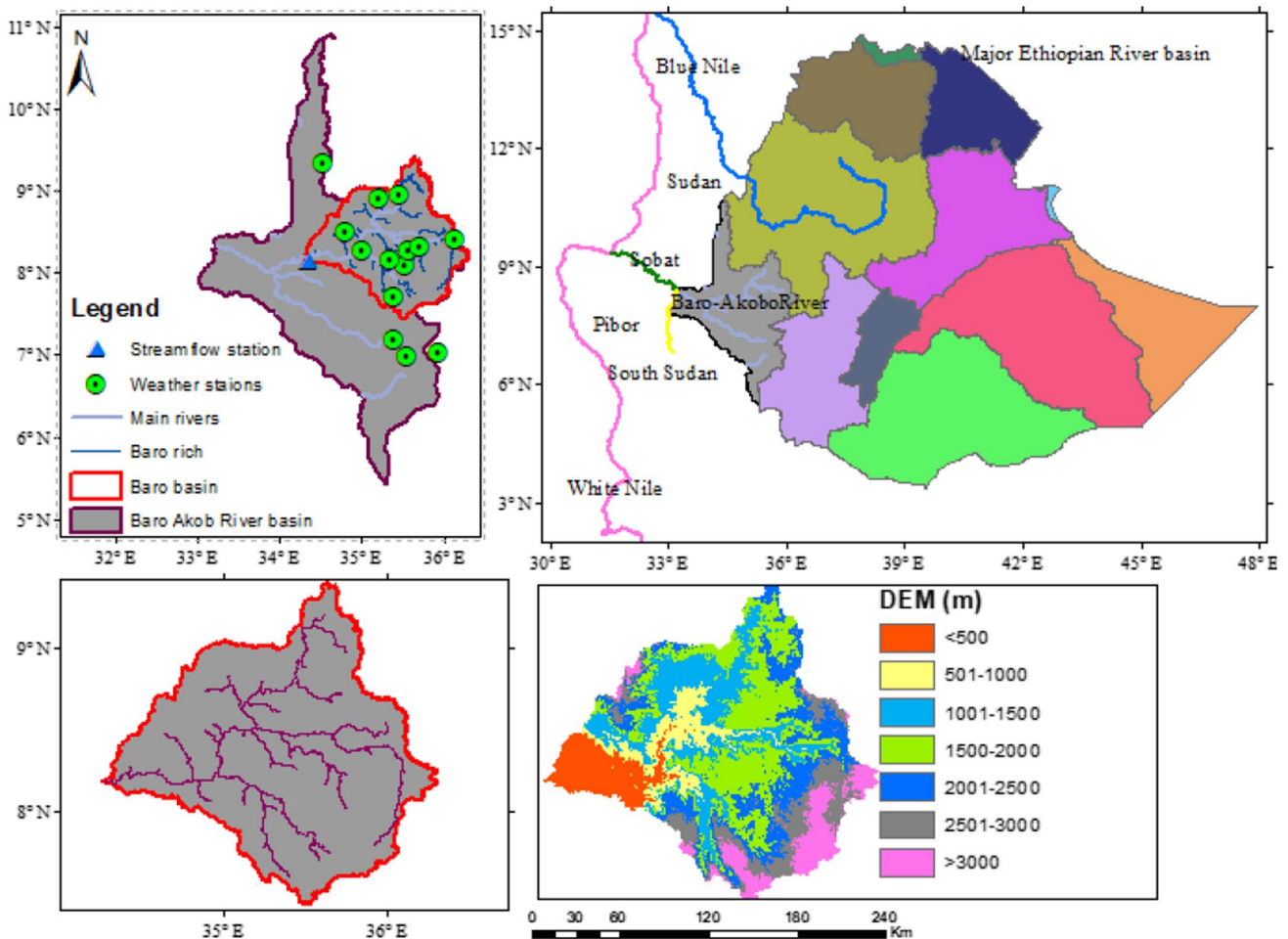


Fig. 1 Location map of the study area including major Ethiopian River basin, weather, and streamflow station. The elevation map is based on a 30 m resolution Digital Elevation Model (DEM)

western highlands of Ethiopia to the Sudanese border to join the White Nile. The study basin covers an area of about 75,912 km² and is located between 5°31' and 10°54' N and 33°00' and 36°17' E. The basin has a complex topography with a significant elevation variation ranging from 389 to 3,266 m. Such complex topography of the basin contributes to a wide-ranging climate, soils, and land use. The basin predominantly has a tropical monsoon climate with distinct wet and dry seasons. Months from March to October represent the wet season, while months from November to February represent the dry season. The basin has immense geopolitical and hydrologic significance for its downstream countries. For instance, the Baro River shares about 83% of the flow with the Sobat River; from June to October (wet season), and it also shares about 14% of its flow with the Nile River basin (Mengistu and Sorteberg 2012). In addition, most of the UNESCO-listed biodiversity sites from Ethiopia are partially or fully found in this basin (UNESCO 2012; Alemayehu et al. 2016).

Data inputs

The SWAT model was used for this study. SWAT requires spatial and temporal data to simulate basin hydrological processes. The spatial data inputs include Digital Elevation Model (DEM), soil map, and land use map. In addition, the temporal data inputs include streamflow, rainfall, maximum and minimum temperatures, relative humidity, solar radiation, and wind speed.

Spatial data

A 30 m × 30 m resolution DEM was acquired from the (USGS) Earth Explorer website (<https://earthexplorer.usgs.gov>). The DEM was used to define the basin boundary and provides important basin properties such as slope gradient, slope length, stream network, and stream characteristics (channel slope, width, and length). The soil physicochemical parameters were acquired from the African Soil Information

System soil data (AfsIS), which provides soil information at 250 m spatial resolution and contains most of the soil parameters for six soil layers (Hengl et al. 2015; Bayabil and Dile 2020). The pedo-transfer function was used to generate the parameters required by the SWAT model (Saxton and Rawls 2006). The dominant soil textural class can be classified as clay, clay-loam, and silt-clay soils. ArcGIS 10.4 software was employed to prepare a raster spatial map of DEM and soil. Land use is another important spatial input data required for the SWAT model setup. It is used to estimate vegetation and their parameters input to the model. The parameterization of the land use classes (e.g., maximum stomatal conductance, maximum root depth, leaf area index, optimal and minimum temperature for plant growth) is based on the available SWAT land use classes (Neitsch et al. 2011). Landsat 7 ETM+ image for the year 2002 was acquired from the (USGS) <http://earthexplorer.usgs.gov/> at a resolution of 30 m. The 2002 land use map was used because good quality observed streamflow data for model calibration (1990–1998) and validation (199–2002) were obtained within this time period. Therefore, it is recommended to use land use data within this time period for reasonable model calibration and validation. Supervised classification methods with a maximum likelihood algorithm (MLC) in ERDAS Imagine software were used for image classification. Supervised classification is a method of classification in which thematic classes are defined by the spectral characteristics of pixels within an image, corresponding to training areas in the field chosen to represent known features. The supervised classification was applied after a defined area of interest (AOI), which is called training classes. More than one training area was used to represent a particular class. The training sites were selected in agreement with Landsat Images and Google Earth. A total of 450 reference data points were acquired from Google Earth imagery. Of the total collected data, 2/3 were used for supervised image classification and the rest 1/3 were used for accuracy assessment. Using the statistical data provided by the training regions, the software attempts

to determine all remaining pixels in the image that fall into these defined classes. In general, the basic sequence operations followed in supervised classification include the defining of training sites, extraction of signatures, and classification of the image. The image was classified into seven land use types, namely forest, agriculture, shrub, grass, urban, wetland, and water (Table 1). All the spatial datasets such as soil and land use were projected to the same projection called the Universal Transverse Mercator (UTM) projection system of Zone 37 N (Fig. 2). To determine the accuracy of land use classification, the users, producers, the overall classification, and the kappa coefficient were estimated using ERDAS Imagine software. The accuracy of classification had an overall classification accuracy of 84.6% and a kappa coefficient of 0.81.

Temporal data

Daily rainfall, maximum temperature (T_{max}), and minimum temperature (T_{min}) for the period 1981–2010 (baseline period) were obtained from the Ethiopian National Meteorological Services Agency (ENMSE). Further descriptions of the weather dataset are available (Mengistu et al. 2021a). Daily observed streamflow data of Baro River (1990–2002) gauge stations were collected from Ethiopian Ministry of Water, Irrigation and Electricity. For stations where there is no observation of solar radiation, sunshine, wind speed, and relative humidity, a gridded dataset from the Climate Forecast System Reanalysis (CFSR) was used. CFSR is designed based on coupled atmosphere-ocean-land surface-sea ice system to provide high resolution and best estimate of climatic variables (Saha et al. 2010; Fuka et al. 2013; Dile and Srinivasan 2014; Mengistu et al. 2021b; Woldeesenbet and Elagib 2021). These temporal climatic and streamflow data were used to calibrate and validate the SWAT model and to develop baseline climate and hydrology.

In addition, the temporal data used include RCM outputs of rainfall and maximum and minimum temperature

Table 1 Land use type with description used in this study

Land use	Description
Forest	Areas covered with dense trees include evergreen forest land, mixed forest, plantation forests, and riparian vegetation. Represents deep to dark red to bright red color in 4, 3, 2 band combination of Landsat image
Shrubland	Areas with shrubs, bushes, and small trees, with little wood, mixed with some grasses. Represents red – brown to bright red in the Landsat image (4, 3, 2 band combination)
Agriculture	Areas used for crop cultivation (irrigated and rain – fed agriculture), fallow land. Represents gray and brown color in 4, 3, 2 band combination of the Landsat image
Urban	Areas of human settlements, roads, artificial surfaces, etc. Represents cyan blue color in 4, 3, 2 band combination of land sat image
Water bodies	Areas permanently covered with standing or moving water such as inland waters, dugouts, and streams. Represents black color in 4, 3, 2 band combination of Landsat image
Wetland	Waterlogged areas, wetlands, and flood plain areas. Represents light red color in 4, 3, 2 band combination of Landsat image

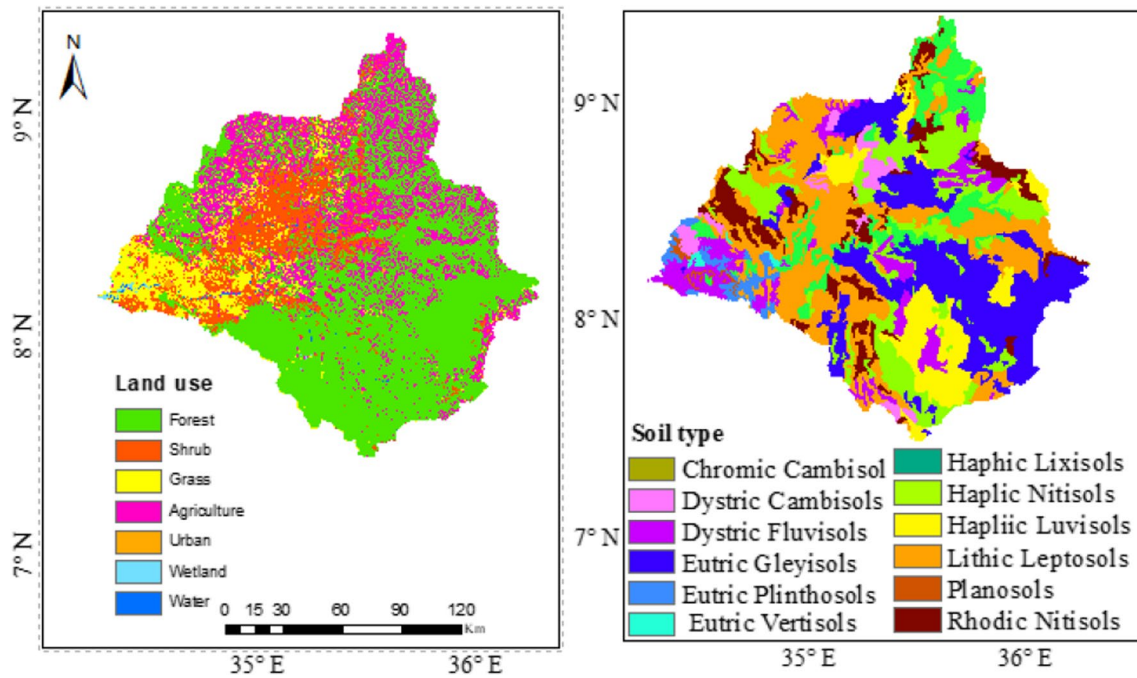


Fig. 2 Land use and soil map of the Baro basin

simulations. The GCM-driven RCM climate projections are provided by the Earth System Grid Federation and downloaded from the Africa-CORDEX data portal (<https://esgf-data.dkrz.de/search/cordex-dkrz/>) with a resolution of 50 km by 50 km. The RCMs (Table 2), namely RCA4 (CNRM), RCA4 (ICHEC), CCLM4 (CNRM), CCLM4 (MPI), REMO (MPI), and their ensemble mean are used because of their good performance in climate simulation in most parts of Africa, including Ethiopia (Nikulin et al. 2012; Fentaw et al. 2018; Dibaba et al. 2019; Mengistu et al. 2021a; Worku et al. 2021). For all RCMs and their ensemble, three-time horizons and two representative concentration pathways (RCP4.5 and

RCP8.5) (Moss et al. 2010) were considered to represent the possible changes in rainfall and temperature. These time horizons include baseline (1981–2010), 2030s (2021–2050), and 2080s (2071–2100).

Statistical bias correction procedures for regional climate model

In data sparse region, several studies used a pixel-to-point approach to evaluate the gridded datasets with the station point dataset (Fenta et al. 2018; Bhattacharya et al. 2020; Mengistu et al. 2021a). The implicit supposition of this approach

Table 2 List of RCMs with their institute and driving GCMs used in the study

RCM	Institute	Driving GCM	Label	Reference
CCLM4	Climate Limited-area Modeling Community (CLMcom)	CNRM-CERFACS-CNRM-CM5	CCLM4(CNRM5)	(Rockel et al. 2008)
CCLM4	Climate Limited-area Modeling Community (CLMcom)	ICHEC-EC-EARTH	CCLM4(ICHEC)	(Baldauf et al. 2011)
CCLM4	Climate Limited-area Modeling Community (CLMcom)	MPI-M-MPI-ESM-LR	CCLM4(MPI)	(Rockel et al. 2008)
RCA4	Swedish Meteorological and Hydrological Institute (SMHI)	CNRM-CERFACS-CNRM-CM5	RCA4(CNRM5)	(Samuelsson et al. 2015)
RCA4	Swedish Meteorological and Hydrological Institute (SMHI)	ICHEC-EC-EARTH	RCA4(ICHEC)	(Samuelsson et al. 2015)
REMO2009	Climate Service Center Germany (CSC) and Max Planck Institute (MPI)	MPI-M-MPI-ESM-LR	REMO2009(MPI)	(Jackob et al. 2012)

is that the rain gauge stations are representative observations of the respective pixels of the RCMs. The climate model data for hydrological modeling (CMhyd) tool obtained from swat.tamu.edu/software/were designed to work with the CORDEX data archive. CMhyd was designed to provide simulated climate data that can be considered representative of the location of the gauges used in a basin model setup. CMhyd is a tool that can be used to extract GCM and RCM data. Therefore, in this study, the historical and future climate model data are extracted for each of the gauge locations using the station's latitude, longitude, and elevation. Then, the average value was used to estimate both the baseline and RCM climate in the basin. Detailed descriptions and information on the theory of linking climate and hydrologic models have been available (Christensen et al. 2008; Teutschbein and Seibert 2012; Rathjens et al. 2016; Kiprotich et al. 2021).

Different bias correction methods, such as linear scaling and distribution mapping methods, show comparable skill in adjusting the mean, standard deviation, and variance of rainfall and temperature events of RCM outputs. Compared to other bias correction methods such as linear scaling and variance scaling methods, the distribution mapping method shows better skill in adjusting the extreme values and wet day probability of RCM outputs with their baseline counterparts (Block et al. 2009; Teutschbein and Seibert 2012; Worku et al. 2020). This study used the CMhyd tool to process the rainfall and temperature bias correction for each station using the distribution mapping methods.

For modifying RCM output, bias correction processes use a transformation algorithm (Piani et al. 2010). Identification of potential biases among the simulated and observed climate variables is the key concept, and it serves as the foundation for modifying control and scenario RCM runs. To change the distribution functions of the modeled variables into the observed ones, the statistical transformations use a mathematical function. Statistical transformations try to find a function h that fits a modeled variable such that its new distribution equals the distribution of the observed variable (Piani et al. 2010; Gudmundsson et al. 2012). These transformations are expressed mathematically as:

$$P_0 = h(P_m). \quad (1)$$

The distribution mapping approach fits the distribution of rainfall and temperature of RCMs with observational data using the Gamma distribution (Gudmundsson et al. 2012) and the Gaussian distributions (Cramér 1999). For instance, the distribution mapping approach provides the following transformation between observed and modeled rainfall:

$$P_0 = F_O^{(-1)}(F_m(P_m)). \quad (2)$$

P_0 is an observed rainfall,

P_m is the model rainfall,

F_m is the CDF related to P_m and

$F_O^{(-1)}$ is the inverse CDF of P_0 .

Hydrological model setup

ArcSWAT 2012.10.24 compatible with ArcGIS 10.4 was used to set up the model. Using the automatic watershed delineation tool in ArcSWAT, basin properties such as slope gradient, slope length, and stream network were extracted from the DEM. A threshold area of 210 km² was used during the SWAT model setup. The HRUs are the smallest modeling units with a similar area of aggregated land use, soil, and slope. Multiple HRU creation approaches were used with a 2, 20, and 10% threshold for land use, soil, and slope units, respectively. The land use, soil and the slope class derived from the DEM were overlaid together to produce 71 sub-basins and 773 HRUs in the basin. Following this spatial data setup, the weather data from each station were used to run the model. The centroid method was used to link the weather station data to the sub-basin (Neitsch et al. 2011; Dile and Srinivasan 2014). The SWAT model estimates the important hydrologic components for each HRUs unit based on the water balance (Eq. 3) and their outputs are aggregated at the basin level to compare the baseline with the future period and scenarios (Neitsch et al. 2011):

$$S_{wt} = S_{wo} \sum_{(i=1)}^t (R_{(day-)} Q_{(surf-)} E_{(a-)} E_{(seep-)} Q_{gw}), \quad (3)$$

where S_{wt} is the soil water content (mm), S_{wo} is the initial soil water content (mm), R_{day} is the amount of precipitation (mm), Q_{surf} is the surface runoff (mm), E_a is the amount of evapotranspiration (mm), E_{seep} is the soil infiltration I (mm), and Q_{gw} is the return flow (mm). In this study, surface runoff was estimated using the curve number (CN) method, potential evapotranspiration was estimated using the Penman–Monteith equation and the channel routing processes were simulated using the Variable Storage Routing method (Neitsch et al. 2011).

To estimate the future climate change impact on the hydrology, a total of five simulation periods were established from the best-performing RCMs (ensemble). Then, the calibrated model is run for a baseline (1981–2010) and for the 2030s (2021–2050) and for the 2080s (2071–2100) periods under the RCP4.5 and RCP8.5 scenarios. The future climate change impact was examined by comparing the monthly, seasonal and annual value of the baseline period with the value of the corresponding future period and climate impact scenarios. The spatial distribution of the waterbalance components such as evapotranspiration and

water yield in the basin were estimated using inverse distance weighting (IDW) method (Bartier and Keller 1996).

Model calibration and validation

Successful application of a hydrologic model depends on parameter sensitivity analysis and model calibration and validation processes. Daily River streamflow data measured at Baro River gauging station (see Fig. 1) were used for model calibration and validation. The model was run for 13 year; the period from 1990 to 1998 was used for calibration, while the period from 1999 to 2002 was used for validation period. The modeling period selection considered good streamflow data availability. The Sequential Uncertainty Fitting version 2 (SUFI2) algorithm in the SWAT Calibration and Uncertainty Program (SWAT-CUP) was used to conduct model parameter sensitivity analysis and calibration (Abbaspour et al. 2015). Eighteen relevant hydrological parameters were chosen for sensitivity analysis (Koch et al. 2012; Mengistu and Sorteberg 2012; Mengistu et al. 2021b), and ten parameters with lower p values and higher t -stats were chosen for calibration and validation. For the sensitivity analysis, parameters related to soil water, runoff, groundwater, and evapotranspiration were taken into account.

The model performance during the calibration and validation period was assessed using suit statistical measures (Moriassi et al. 2007). These statistical measures include the Nash–Sutcliffe Efficiency (NSE) (Eq. 4), Coefficient of Determination (R^2) (Eq. 5), and Percent bias (PBIAS) (Eq. 6):

$$\text{NSE} = 1 - \frac{\sum_{i=1}^n (O_i - S_i)^2}{\sum_{i=1}^n (O_i - \bar{O})^2}, \quad (4)$$

$$R^2 = \frac{\left[\sum_{i=1}^n ((O_i - \bar{O})(S_i - \bar{S})) \right]^2}{\sum_{i=1}^n (O_i - \bar{O})^2 \sum_{i=1}^n (S_i - \bar{S})^2}, \quad (5)$$

$$\text{PBIAS} = \frac{\sum_{i=1}^n (O_i - S_i)}{\sum_{i=1}^n (O_i)} \times 100, \quad (6)$$

where O_i is the observed streamflow (m^3/sec), \bar{O} is the mean measured streamflow (m^3/sec), S_i is the simulated streamflow (m^3/sec), and \bar{S} is the mean simulated streamflow (m^3/sec) and n is the number of observations. According to Moriassi et al. (2007), the SWAT model is acceptable when the NSE and R^2 are greater than 0.5 and the PBIAS varies between ± 15 to 25%. Besides, SUFI-2 is used to measure uncertainty in terms of p -factor and r -factor, which is

expressed in terms of the 95% prediction uncertainty (95 PPU) (Abbaspour et al. 2007).

Indicators of hydrologic alteration

In addition to SWAT, in this study, the hydrological parameters were estimated using the IHA 7.1 software (The Nature Conservancy 2009). The software and method required at least 20 years of daily hydrological data, which include streamflow, river stages, and groundwater levels (Richter et al. 1996). However, in this study, we have used the daily streamflow data to compare the pre-impact (baseline) against post-impact (future periods and scenarios). For IHA setup, daily streamflow data for the baseline period (1981–2010) were regarded as natural flow and the future period and RCPs climate scenarios as altered flow. A comparable approach has been applied in other studies (Kiesel et al. 2019; López-Ballesteros et al. 2020; Woldesenbet 2022). The IHA enables the user to conduct a comparison analysis called the Range of Variability Approach (RVA) that practically evaluates the hydrologic alteration at a particular river site before and after an impact or between different long periods. RVA distributes the full range of pre-impact data for each parameter into three categories of equal range (low, middle, and high). The low category defines values below or equal to the 33rd percentile of the median, the middle defines values found between the 34th to 67th percentile, and the high defines values that are greater than the 67th percentile. The expected frequency with which the “post-impact” values would fall within each class is calculated using Eq. 7:

$$\text{HA} = \frac{\text{Observed frequency} - \text{Expected frequency}}{\text{Expected frequency}}. \quad (7)$$

A positive hydrological alteration (HA) value indicates that the frequency of values in the category has increased from the pre-impact (baseline) to the post-impact (future periods and scenarios) (with a maximum value of infinity), whereas a negative value indicates that the frequency of values has decreased (with a minimum value of -1) (Richter et al. 1996).

Results

Performance of regional climate model

The performance of the bias-corrected RCMs and their ensemble mean to simulate the basin climate using Taylor’s diagram method are presented in Fig. 3. A comparison of the various bias-corrected RCM simulations with the baseline data using Taylor’s diagram shows that the ensemble has

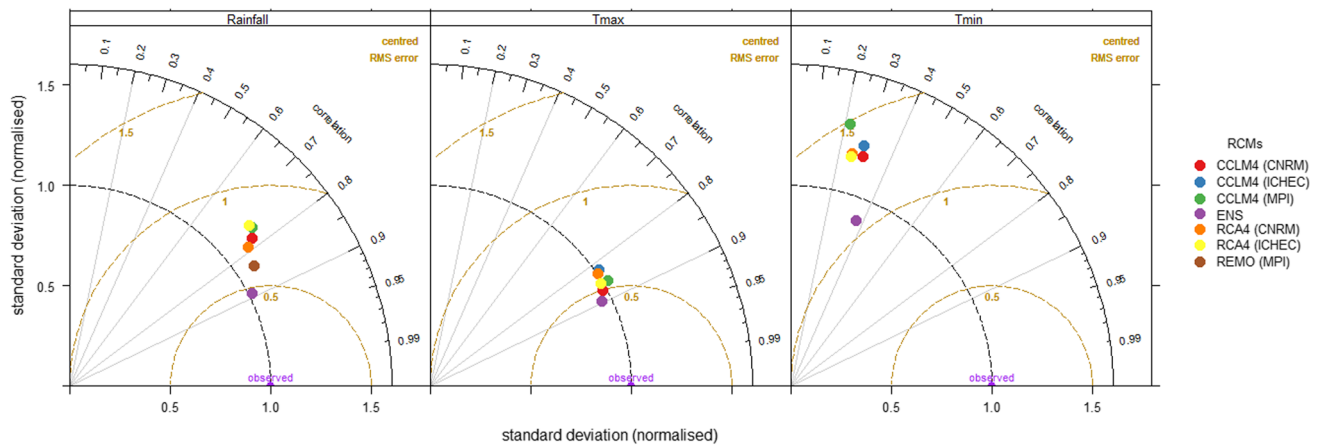


Fig. 3 The performance of the bias-corrected regional climate models and their ensemble mean for monthly rainfall, and maximum and minimum temperatures as represented by Taylor's diagram

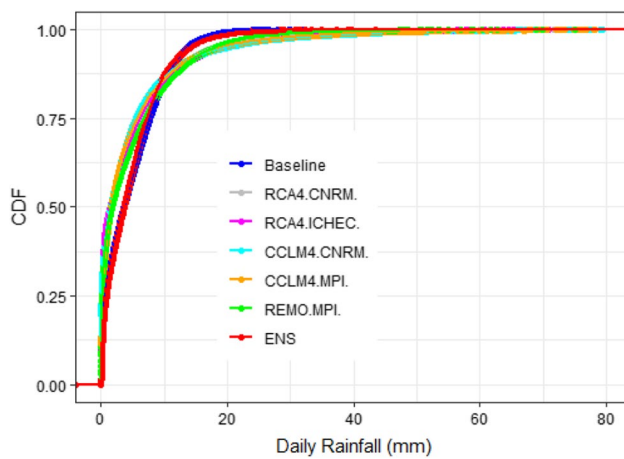


Fig. 4 Comparison of the Cumulative Distribution Function (CDF) of the different RCM simulations of rainfall estimates with baseline climate

relatively better performance, while the CCLM4 (MPI) performance is low. The high correlation values and the lower RMSE and standard deviation values show the better performance of the ensemble in the Baro–Akobo River basin climate simulation. For rainfall and T_{\max} , the points of the ensemble mean are closer to the baseline compared with the individual models, with R close to 1. On the other hand, the RMSE of the ensemble mean is also close to 0 compared with the other individual models.

In addition to the Taylor diagram, a visual inspection of Fig. 4 shows that the bias-corrected cumulative distribution function (CDF) of the baseline daily rainfall is best captured when using model ensembles instead of individual models. For instance, in simulating the 75% percentile, approximately less than or equal to 7.7 mm/day was estimated from the baseline, a slightly lower rainfall amount of 7.2 mm/day

from the ensemble, and the CCLM4 (CNRM) was estimated as low as 5.6 mm/day. While in estimating the 95% percentile, all models, including the ensemble, overestimated the baseline. Approximately less than or equal to 13.3 mm/day was estimated from the baseline, a slightly higher rainfall amount of 14 mm/day from the ensemble, and CCLM4 (CNRM) was estimated as large as 20.5 mm/day.

These statistical comparisons suggest that climate change impact studies in the basin may benefit from using an ensemble of simulated rainfall and temperatures as obtained from multiple regional climate models instead of simulated rainfall from individual models. Other studies comparing the historical performance of RCMs also show that multimodal ensembles often perform better than individual RCMs with higher correlation and lower biases, standard deviations, and RMSE (Teutschbein and Seibert 2010; Taylor et al. 2012; IPCC 2014; Mengistu et al. 2021a; Worku et al. 2021).

Rainfall and temperature projection under future periods and climate scenarios

The future period projection of the mean monthly rainfall and T_{\max} and T_{\min} simulated by bias-corrected RCMs and their ensemble is presented in Figs. 5 and 6, respectively. The projected mean monthly rainfall for the 2030s and 2080s under both climate scenarios did not show a consistent magnitude and direction compared with the baseline climate. The projected rainfall for most of the RCMs shows a decreasing trend in the majority of the months of the year under the future period and scenarios. For the RCP4.5 scenarios, monthly rainfall changes range from -61 to 52% and -63 to 41% for the 2030s and 2080s, respectively. Both the largest decrease of 63% and an increase of 52% are estimated by RCA4 (CNRM). Similarly, for RCP8.5 scenarios, monthly rainfall changes range from -54 to 69% and -65

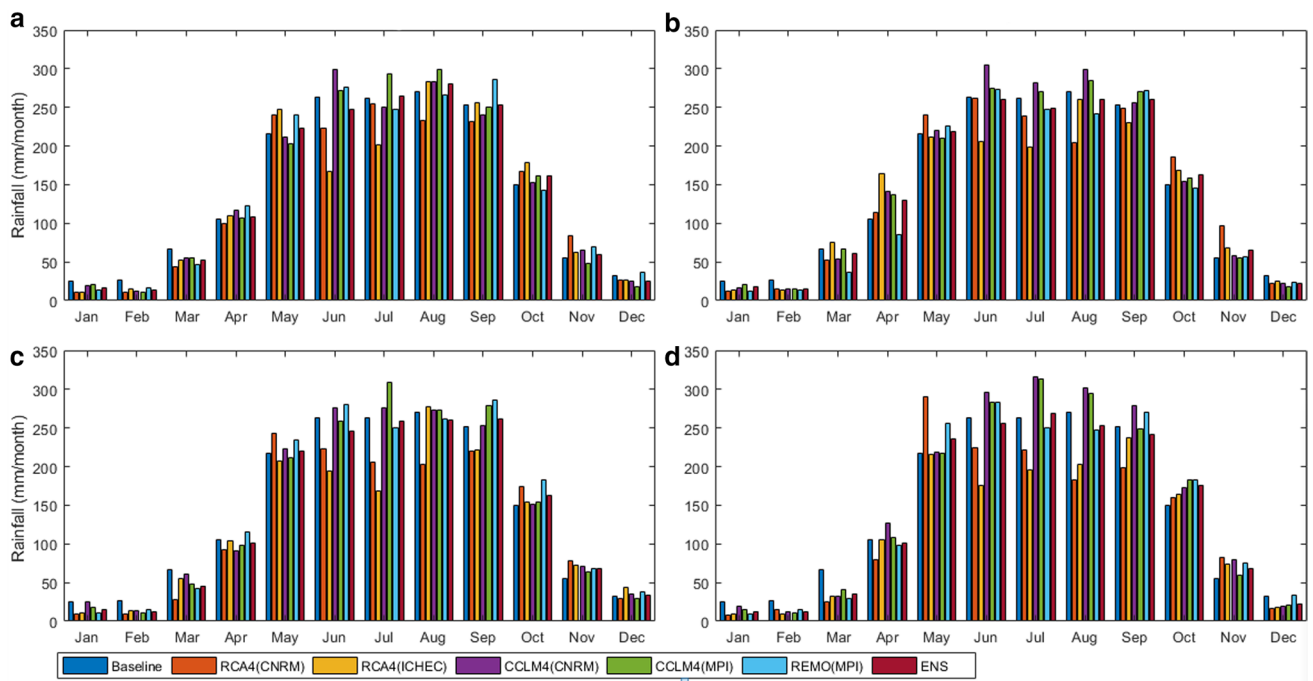


Fig. 5 Long-term mean monthly rainfall for the baseline and future period and scenarios: **a** RCP4.5 2030s, **b** RCP8.5 2030s, **c** RCP4.5 2080s, and **d** RCP8.5 2080s

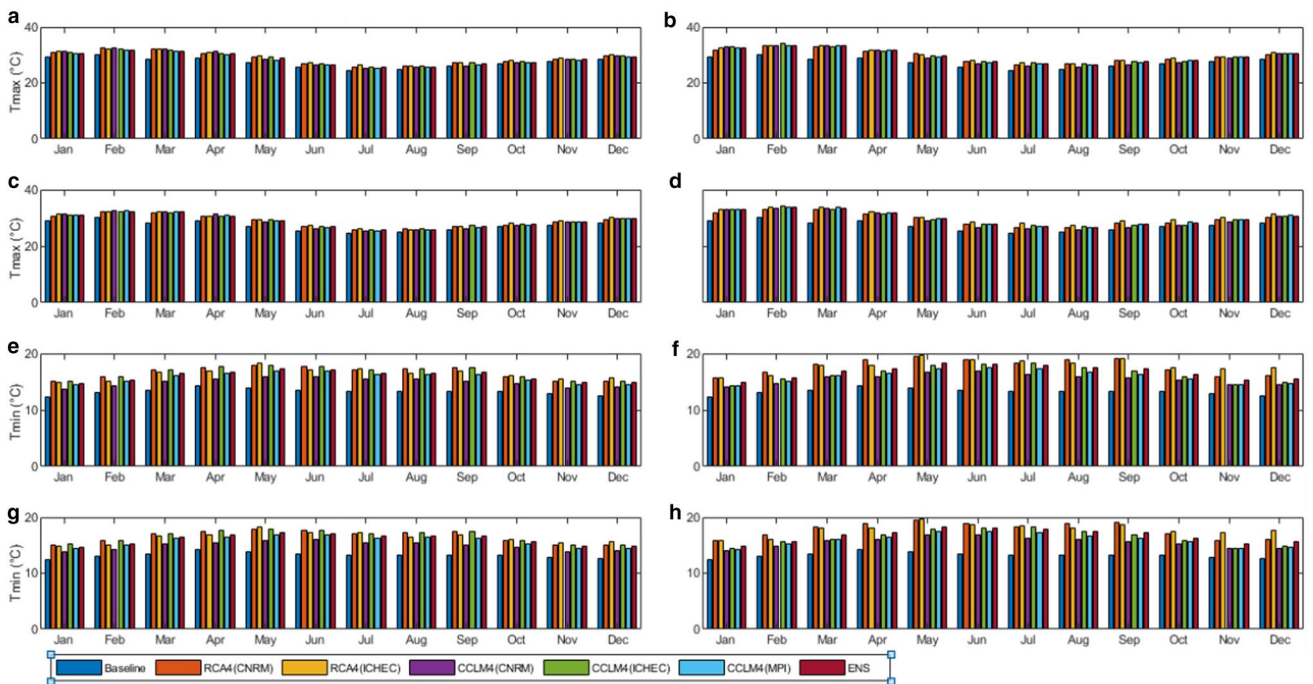


Fig. 6 Long-term mean monthly temperature for the baseline and future period and scenarios. The first four panels **a**, **b**, **c**, and **d**, and the next four panels **e**, **f**, **g**, and **h** represent RCP4.5 2030s, RCP8.5

2030s, RCP4.5 2080s, and RCP8.5 2080s for maximum temperature (°C) and minimum temperature (°C), respectively

to 50% for the 2030s and 2080s, respectively. The largest decrease of 65% and an increase of 69% are estimated by the

RCA4 (ICHEC) and RCA4 (CNRM) models, respectively. The typical dry rainfall months (January and February) show

a consistent decreasing trend for all RCMs under future periods and scenarios, while from October to December, the majority of the RCMs show an increasing trend. For the RCP8.5 scenario, dry season rainfall changes from -25 to 4% and -33 to -4% for the 2030s and 2080s, respectively. Wet season rainfall for the RCP8.5 scenario ranges from -3.7 to 7.8% and -15% to 2.4 for the 2030s and 2080s, respectively, demonstrating a relatively narrower range of projection for the wet season than the dry season.

In general, there is much better consistency between climate model projections of temperature than rainfall. All bias-corrected RCMs show a consistent increase in T_{\max} and T_{\min} as projected by RCP4.5 and RCP8.5 throughout the future period. For example, CCLM4 (ICHEC) under RCP8.5 shows the largest increase of 3.9 °C in T_{\max} in February by the 2080s, whereas CCLM4 (MPI) under RCP4.5 for the 2030s indicates the lowest increase in T_{\max} of 0.52 °C in July. Similarly, RCA4 (ICHEC) shows the highest increase T_{\min} of 5.34 °C in May under RCP8.5 for the 2080s, whereas the CCLM4 (CNRM) model indicates the lowest increase of 1.39 °C in January under RCP4.5 for the 2030s. These results show a change in both T_{\max} and the T_{\min} for the 2080s is larger when driven by RCP8.5 compared to RCP4.5 and the increase for T_{\min} is larger than T_{\max} .

In this study, the ensemble mean was used for the projection of the impact of climate change scenarios on rainfall and temperatures on the hydrology of the basin. Figure 7 depicts the change in projected ensemble monthly rainfall and minimum and maximum temperatures under the RCP4.5

and RCP8.5 scenarios. The extent of changes and directions in the ensemble mean monthly rainfall varies, with the largest decrease of 41% in February under RCP8.5 for the 2080s and the largest increase of 22% in November under RCP4.5 for the 2080s. Further, the dry and wet season mean rainfall is expected to decrease by up to 19% and 4% , respectively, under RCP8.5 by the 2080s. This indicates a relatively narrower range of projections for the wet season than for the dry season. The decrease will be up to 5.1% for annual rainfall compared to the baseline period, which is expected under RCP8.5 by the 2080s scenarios. The projected T_{\max} and T_{\min} under the RCP4.5 and RCP8.5 scenarios showed an increasing mean value for both future periods. The mean annual T_{\max} is expected to rise by 1.2 to 1.6 °C under RCP4.5 and by 2.4 to 2.6 °C under RCP8.5. Similarly, RCP4.5 would cause the mean annual T_{\min} to rise by 2.2 to 2.6 °C, while RCP8.5 would cause it to rise by 3.26 to 3.29 °C.

Hydrological model sensitivity, calibration, and validation

Different hydrologic parameters (Table 3) of the basin were evaluated for their sensitivity during the calibration processes. Based on the global sensitivity analysis, CN2 (Curve number), soil evaporation compensation factor (ESCO), and soil depth (SOL_Z) were recognized to be the most sensitive parameters. As a result, a slight change in these parameters has a rapid response in runoff generation because these parameters depend on several factors,

Fig. 7 Projected changes in mean monthly, seasonal, and annual ensemble future climate and scenarios compared to the baseline condition



such as soil types, soil permeability, and land use type. Groundwater "revap" coefficient (GW_REVAP), maximum canopy storage (CANMX), and base-flow alpha-factor (ALPHA_BF) were all identified to have a substantial impact on the calibration processes of the hydrological

components. In general, the higher the *t*-stat and the lower the *p* value (Fig. 8), the more the parameter is sensitive in simulation (Abbaspour et al. 2015).

The model calibration and validation show a reasonable agreement in terms of NSE, *R*², and PBIAS as well as

Table 3 The most sensitive parameters identified during the calibration period using observed daily streamflow

List of parameters	Description	Range	Final value
R_CN2.mgt	Curve number	± 25%	0.07
V_ALPHA_BF.gw	Base-flow alpha-factor (Days)	0–1	0.3
V_ESCO.hru	Soil evaporation compensation factor	0–1	0.41
R_SOL_AWC(..).sol	Soil available water capacity (mm/mm)	± 25%	−0.03
V_GW_REVAP.gw	Groundwater "revap" coefficient	0.02–0.2	0.11
V_EPCO.hru	Plant uptake compensation factor	0–1	0.67
R_SOL_Z(..).sol	Soil depth (mm)	± 25%	0.05
V_CANMX.hru	Maximum canopy storage (mm)	0–10	4.55
R_SOL_K(..).sol	Soil saturated hydraulic conductivity (mm/hr)	± 25%	0.04
R_SOL_BD.sol	Moist bulk density	± 25%	0.09

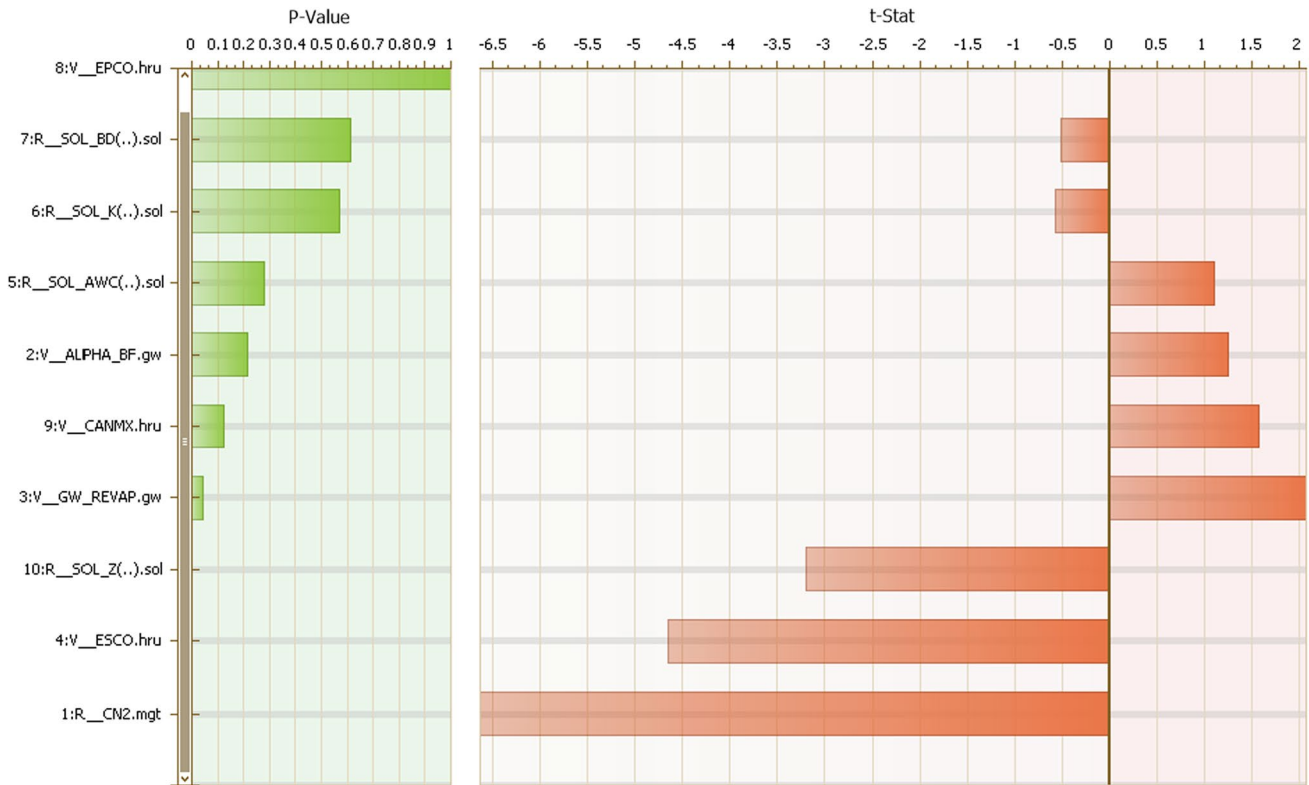


Fig. 8 Global sensitivity analysis for daily streamflow simulation for the Baro River station

Table 4 Performance measure values of the SWAT model to simulate streamflow during the calibration and validation period

Period	Daily					Monthly				
	<i>R</i>	NSE	PBIAS	<i>p</i> -factor	<i>r</i> -factor	<i>R</i>	NSE	BIAS	<i>p</i> -factor	<i>r</i> -factor
Calibration	0.73	0.73	− 4	0.71	0.49	0.9	0.89	− 0.9	0.75	0.5
Validation	0.8	0.79	1.7	0.7	0.53	0.87	0.85	− 2.4	0.72	0.4

the uncertainty analysis of p -factor and r -factor (Table 4). However, the daily period statistical evaluation was weaker than those computed for the monthly period. For example, considering the objective function for optimization, the daily NSE values were 0.73 and 0.8, while the monthly values were 0.89 and 0.85 for the calibration and validation period, respectively. In general, results show that the SWAT model can reasonably simulate the hydrological characteristics of the basin (Moriassi et al. 2007). Similarly, the uncertainty analysis for the monthly simulation was better than the daily simulation. The streamflow simulation also provided acceptable prediction uncertainty (p -factor and r -factor) estimates for both daily and monthly periods (Abbaspour et al. 2015).

In addition, Fig. 9 shows the hydrograph of monthly and daily streamflow observations with the SWAT model simulation. The model best captured the streamflow hydrograph in terms of timing and magnitudes of flow, but the model did not capture the peak flow very well. Moreover, the simulation accuracy of monthly flow is relatively better than the daily simulations. The results have good agreement with the previous study (Mengistu and

Sorteberg 2012). Therefore, the SWAT model could best capture the future hydrology of the Baro–Akobo basin.

Streamflow response under future periods and climate scenarios

The influence of the future climate on the streamflow was assessed at monthly, annual, and seasonal time scales. Table 5 presents the response of streamflow under RCP4.5 and RCP8.5 scenarios. The estimate shows that the projected average monthly, seasonal, and annual streamflow is expected to decrease compared to 1981–2010, the baseline period. The mean of the results indicates decreases in streamflow in the ranges of –11 to –68% for monthly flows, –26 to –39% for dry season flows, –28 to –41% for wet season flows, and –28 to –40% for annual flows. The highest decreasing change was observed during April under the RCP8.5 2080s, the lowest was during September under the RCP4.5 2030s.

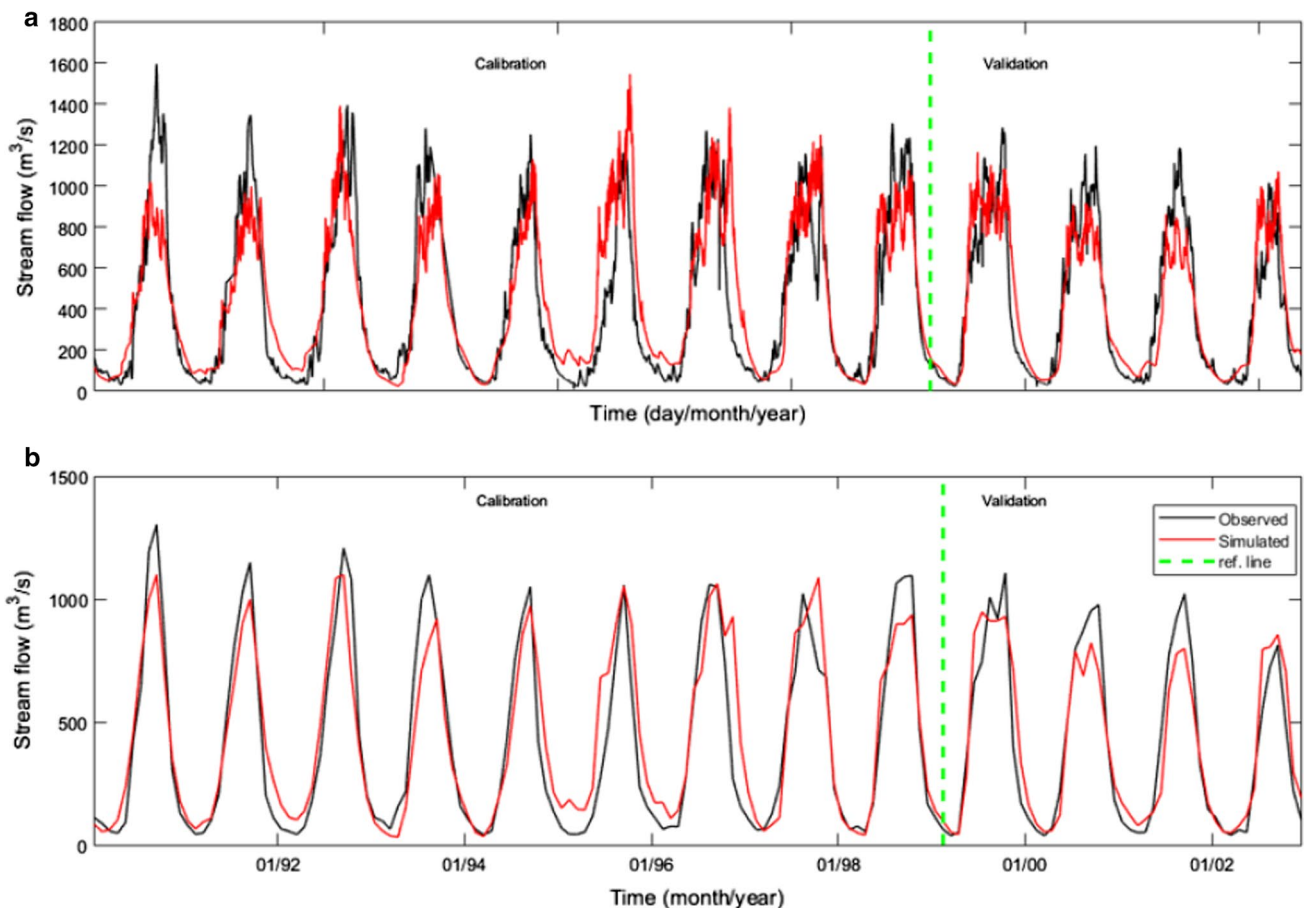


Fig. 9 Observed and simulated streamflow for the calibration and validation period for Baro River station: **a** daily and **b** monthly time scale

Water balance response under future periods and scenarios

Water balance refers to the net amount of water contributed by sub-basins and HRUs to the streamflow. To understand more about the future water resource availability, a water balance analysis was performed on an annual basis using the hydrological components as simulated by the SWAT model (Table 6 and Figs. 10 and 11). The projected results showed that there is a substantial decrease in surface runoff, total aquifer recharge, and total water yield for the ensemble

mean of RCP4.5 and RCP8.5. In contrast, projected climate change for both RCPs will increase evapotranspiration, particularly for RCP8.5 2080s.

Evapotranspiration is likely to increase due to a rise in temperature both spatially and temporally. Though there is a difference in magnitude, evapotranspiration showed an increasing trend under all the future climate scenarios. The highest increase in evapotranspiration (14.2%) was predicted in the 2080s under the RCP8.5 climate scenario (Table 6). In addition, the spatial distribution of evapotranspiration (Fig. 10) shows the forest cover-dominated area in higher

Table 5 Percentage of changes in projected mean monthly, seasonal, and annual ensemble streamflow compared to the baseline climate

Period	Jan	Feb	Mar	Apr	May	Jun	Jul	Aug	Sep	Oct	Nov	Dec	Dry season	Wet season	Annual
RCP4.52030 s	-37	-54	-64	-62	-60	-41	-31	-18	-11	-21	-20	-33	-30	-28	-28
RCP8.52030 s	-33	-54	-58	-58	-53	-38	-34	-20	-19	-19	-12	-35	-26	-29	-28
RCP4.52080 s	-44	-58	-63	-64	-60	-47	-37	-26	-29	-22	-28	-41	-37	-35	-35
RCP8.52080 s	-47	-62	-64	-68	-62	-57	-41	-38	-31	-27	-27	-49	-39	-41	-40

Table 6 Percentage of changes in projected mean annual ensemble water balance compared to the baseline climate

Period/scenarios	ET	SW	PERC	SURQ	GWQ	WYLD	LATQ
Baseline	793	306	282	466	235	827	111
RCP4.52030 s	10.3	-0.7	-44.6	-48.1	-9.5	-31.5	-11.2
RCP8.5 2030s	11.8	-0.8	-45.2	-47.5	-10.8	-31.5	-11.0
RCP4.5 2080s)	12.5	-1.3	-45.2	-50.7	-25.6	-38.3	-15.6
RCP8.5 2080s	14.2	-2.2	-45.2	-54.0	-41.3	-45.4	-18.9

Fig. 10 Mean annual actual evapotranspiration (mm) under baseline and future climate scenarios in each sub-basin: **a** Baseline (1981–2010), **b** RCP4.52030 s, **c** RCP8.52030 s, **d** RCP4.52080 s, and **e** RCP8.5 2080s climate scenarios

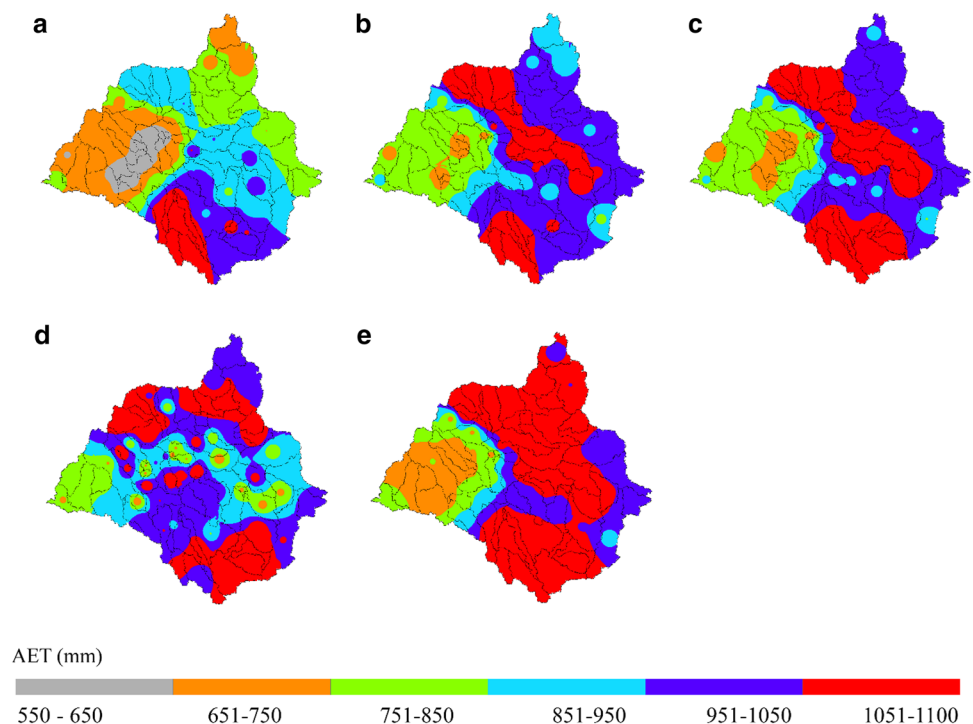
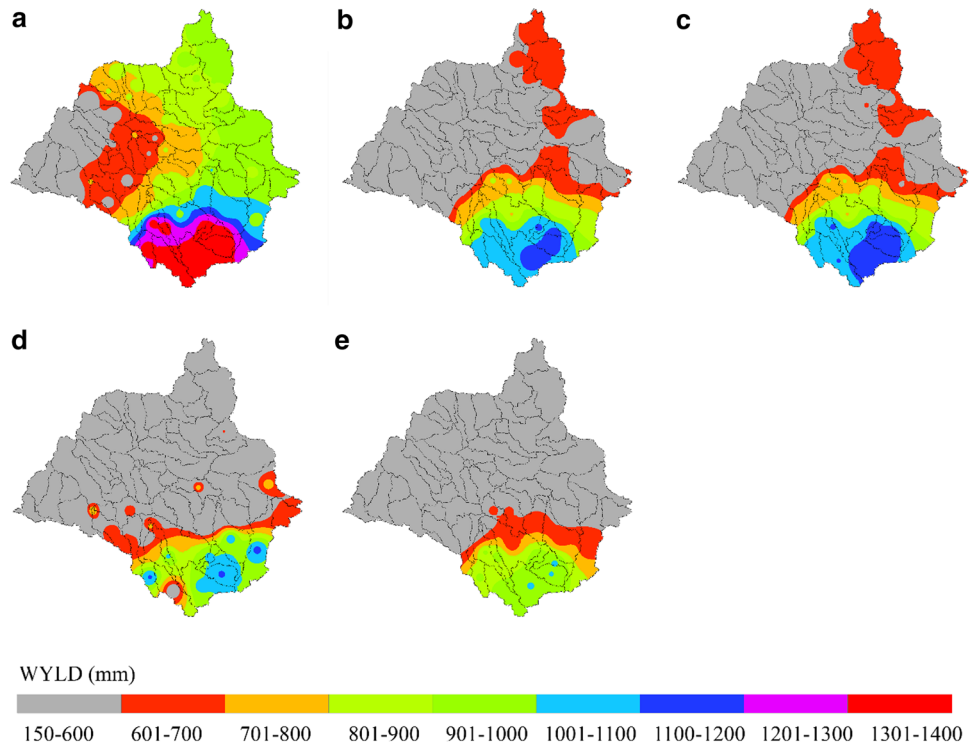


Fig. 11 Mean annual water yield (mm) under baseline and future climate scenarios in each sub-basin: **a** Baseline (1981–2010), **b** RCP4.5 2030s, **c** RCP8.5 2030s, **d** RCP4.5 2080s, and **e** RCP8.5 2080s climate scenarios



elevations is more susceptible to evapotranspiration in the basin.

The water yield in the SWAT model includes direct surface runoff, groundwater flow, lateral flow, transmission losses, and pond abstraction. Figure 11 depicts the spatial variation in water yield under RCP4.5 and RCP8.5 for different time horizons. The water yield in the SWAT model includes direct surface runoff, groundwater flow, lateral flow, transmission losses, and pond abstraction. In comparison with rainfall and temperature, other parameters like wind speed, solar radiation, and relative humidity have less effect on water yield. Unlike evapotranspiration, water yield is likely to decrease due to a rise in temperature and a decrease in rainfall both spatially and temporally. Water yield is projected to be decreased by 16.7% in the 2030s under the RCP4.5 scenario, and the decrease will be by 40.8% under RCP8.5 in the 2080s. For the baseline climate, water yield is higher in the higher reaches of the basin where rainfall is higher as compared to the lower reaches of the basin.

Indicators of hydrological alteration under future period and climate scenarios

The median monthly flow simulation from the indicators of hydrological alteration shows a decreasing trend for all months of the year (Fig. 12). Compared to the RCP4.5 scenarios, the RCP8.5 2080s is the most altered scenario based on the median value. The reduction in the stream flow can be attributed to the increase in temperatures and a decrease in rainfall. This result

is in agreement with other studies on climate change in Greece (López-Ballesteros et al. 2020). They projected a decrease in the monthly and seasonal flows under future climate scenarios of RCP4.5 and RCP8.5.

The hydrological flow indicators related to monthly flows presented a decrease in the high and middle RVA categories. This means a decrease in the frequency of observed values compared to the lower RVA limit. Unlike the high and middle categories, the majority of the indicators related to monthly flows showed an increase in the low RVA category, which means an increase in the frequency of observed values than the upper RVA limit (Fig. 13). Furthermore, Fig. 13 depicts the annual 1-, 3-, 7-, 30-, and 90-day maximum flows, which show a decrease in the high and middle RVA categories while increasing the low RVA category for the majority of the scenarios tested. Similarly, annual 1-, 3-, 7-, 30-, and 90-day minimum flows showed a decrease in the high and middle RVA categories while increasing in the low RVA category. Besides, results also indicated a decrease in the high and middle RVA categories for the duration of the low and high pulse events, but an increase in the low RVA category was projected.

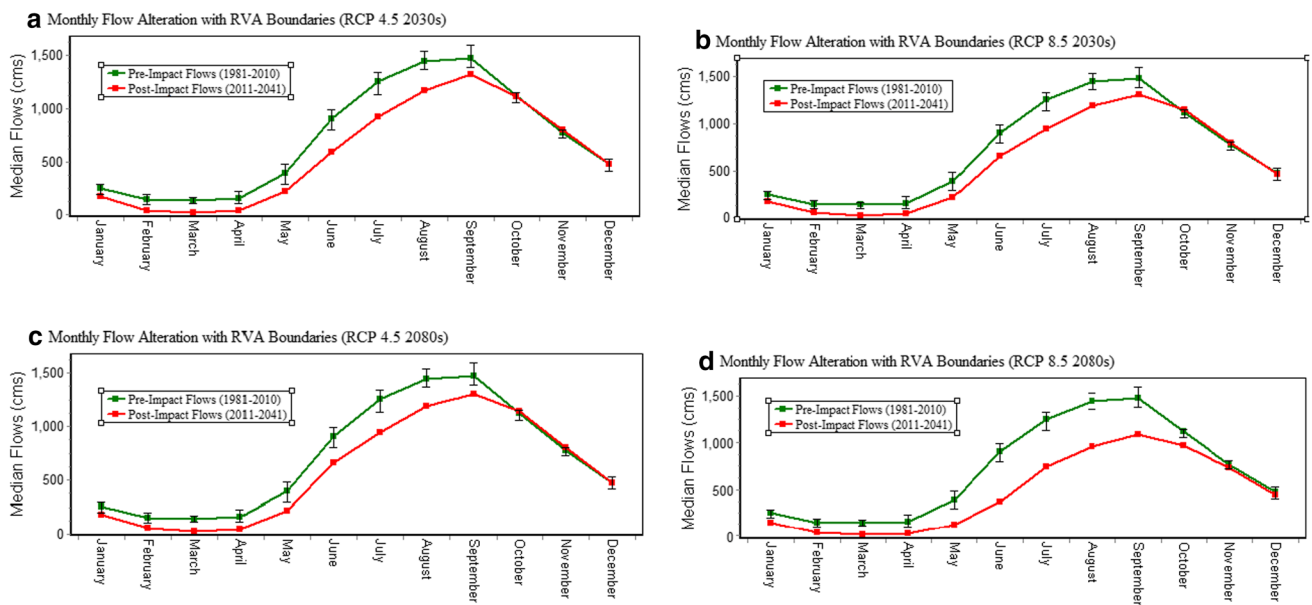


Fig. 12 Monthly median streamflow for baseline conditions and future periods and scenarios for Baro River stations

Discussion

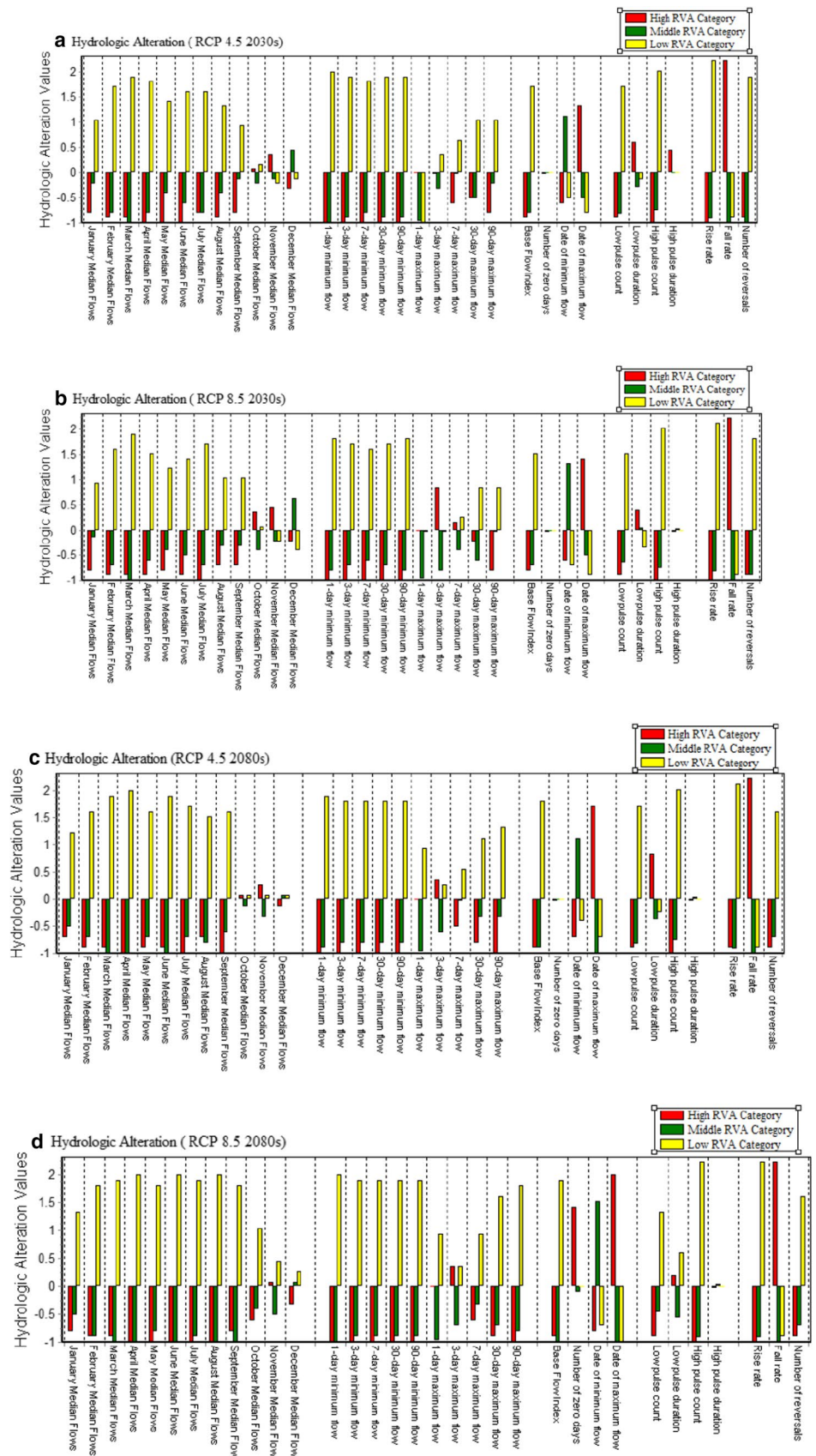
Climate change under future periods and climate scenarios

The bias-corrected individual RCMs as well as the ensemble temperature projection show good consistency with the projected global climate scenarios compared to the rainfall. However, in general, the climate projections show uncertainty in both rainfall and temperature projections in the future period and scenarios. The greater difference in the directions and magnitudes in RCM projections, particularly for rainfall, demonstrates a wide range of uncertainties associated with future rainfall projections. This result is consistent with other studies Hawkins and Sutton (2011) found that future period climate projections are inconsistent under different RCMs and RCPs, suggesting large uncertainty in the projection of climate, particularly in rainfall. According to Kundzewicz et al. (2018), the main sources of uncertainty in future climate projections are uncertainty in the future amount of greenhouse gas emissions and uncertainty related to the inadequate model representation of climate processes. Beyene et al. (2010) predicted a wide range of individual GCM rainfall projections. Their finding under the A2 emission scenario shows that the Nile River basin will experience a substantial decrease in December to February rainfall changes ranging from -24 to 37% and -40 to 18% for the periods 2010–2039 and 2070–2099, respectively, which is somewhat comparable to our -25 to 4% and -33 to -4% for the periods 2030s and 2080s for the RCP8.5 scenario

projection, respectively. Similarly, their findings show that the June to August rainfall for the entire Nile basin under the A2 emissions scenario varies from -21 to 34 and -42 to 15% for the periods 2010–2039 and 2070–2099, respectively. Their finding of a relatively narrower range of projection for June to August than for December to February is comparable to our seasonal rainfall projection. According to the IPCC (2001), based on nine GCMs, the Nile basin will experience rainfall changes of between 0 and 40 by the end of the twenty-first century. In contrast, Worqlul et al. (2018) have projected an increase in the dry season rainfall in the upper Blue Nile basin using the downscaled outputs of the HadCM3 climate model. Eastern and tropical Africa could show a 7% rise in rainfall (IPCC 2007). Findings in the IPCC Third Assessment by McCarthy et al. (2001) showed that the predicted future changes in mean monthly and seasonal rainfall in Africa are not well defined. The diversity of African climates, particularly the high rainfall variability and inadequate meteorological stations, makes the projection of future rainfall challenging at sub-regional and local scales. Therefore, such climate model comparison is crucial for future climate impact studies, and the selection of the best-performing model could reduce the uncertainty.

Because of the uncertainty among climate models, the ensemble mean is undertaken to obtain a generalized picture of the future climate and its hydrological impacts. The finding indicated that the difference in mean seasonal and annual rainfall is less than the difference in monthly rainfall. The decrease will be up to 5% for annual rainfall compared to the baseline period, which is expected under RCP8.5 2080s.

Fig. 13 Values of hydrologic alteration within each RVA category for the baseline conditions and future periods and scenarios



The finding of the ensemble mean is consistent with (Dibaba et al. 2020; Worku et al. 2021), who showed a decreasing annual rainfall projection under bias-corrected RCP4.5 and RCP8.5 scenarios in the Ethiopian highland. In addition, the temperature projection shows a higher increase in T_{\min} than T_{\max} under future periods and scenarios. The temperature projections show strong consistency with other studies conducted in Ethiopia and the global temperature predictions. Several studies in Ethiopia, such as Elshamy et al. (2009), Setegn et al. (2011), Woldeesenbet et al. (2018), Worqlul et al. (2018), and Muleta (2021) indicated an increase in temperatures as compared to historical observations. Furthermore, according to the endorsement of the (IPCC 2013), a higher increase in temperature is predicted in the 2080s than in the 2030s future period. In other studies in Africa, Hulme et al. (2001) indicated that during the twentieth century, mean annual temperatures increased by 20 °C, whereas mean annual rainfall decreased by 20%. The risks associated with extreme events in the climate are found to be high, with an extra 1 °C increase in warming. All these results demonstrate there will be a high rise in temperature unless considerable and sustainable actions are taken to limit greenhouse gas emissions.

Hydrological impact under future periods and scenarios

After calibrating the SWAT model, future climate impacts are projected using the ensemble of rainfall, T_{\max} , and T_{\min} . The decrease in rainfall, combined with an increase in temperature, will result in a decrease in seasonal and annual streamflow. Though the predicted climate change for both RCPs will lead to a decrease in streamflow in the river, the decrease will be greater for RCP8.5 in the 2080s than in the 2030s. The decrease in streamflow under the RCP8.5 scenario is in agreement with other previous studies in other parts of Ethiopia (Dibaba et al. 2020; Worku et al. 2021). The finding is also consistent with Beyene et al. (2010), who showed the Nile River is expected to decline in 2040–2069 and 2070–2099 due to the decline in rainfall and increased evaporation demand. Therefore, greater streamflow reduction by the 2080s, particularly under the RCP8.5 scenario, indicates a challenge to future water availability if climate change mitigation is not applied. The projected decrease in streamflow rates will harm many sectors, including aquatic ecosystems, domestic, irrigation, and hydropower water use. Results of the current study indicated the necessity of employing sustainable water management strategies, which are needed ahead of future expected changes in the climate.

Water balance analysis also indicates that the decrease in rainfall combined with an increase in temperature in the future will result in a decrease in surface runoff, water yield, and groundwater, but an increase in evapotranspiration. The

spatial distribution of evapotranspiration also shows that the area under forest cover dominated at higher elevations is more susceptible to changes in evapotranspiration in the basin. The projected increase in ET, particularly in the forest cover area, can be attributed mainly to the forest land consuming more water compared to other land use types such as grassland. Similarly, the water yield is higher in the higher reaches of the basin where rainfall is higher as compared to the lower reaches of the basin. The increase in evapotranspiration and the decrease in surface runoff, water yield, and groundwater in the future period and RCP4.5 and RCP8.5 climate scenarios are consistent with other studies conducted in the Ethiopian highland (Dibaba et al. 2020; Worku et al. 2021). Research output shows that the decrease in rainfall and the increase in both T_{\max} and T_{\min} due to climate change may have a great impact on soil water balance by increasing evapotranspiration, thereby impacting crop development and agricultural productivity (Kang et al. 2009). Research by Liu et al. (2022) showed that under continued greenhouse gas emissions, global agricultural water shortages will exacerbate up to 84% of cropland between 2026 and 2050. Such a decrease in future water availability in the basin may lead to widespread impacts on the basin's agricultural, domestic, and livestock water supply and other ecosystem services. Therefore, consideration should be given to irrigation infrastructure design. Additionally, a larger storage facility is required to offset the decrease in water yield and surface runoff due to the decrease in rainfall.

The hydrological impact of climate change in the basin estimated by the IHA also shows a decrease in streamflow in the 2030s and 2080s under the RCP4.5 and RCP8.5 scenarios compared to the baseline period. The largest streamflow change is produced for RCP8.5 in the 2080s simulation. A positive hydrologic alteration value indicates increased frequency (from baseline to future), while negative values correspond to decreased frequency. The IHA study outputs on streamflow projections for the basin are consistent with previous studies on the impact of climate change in Greece (López-Ballesteros et al. 2020). Their result shows that the decrease in the monthly and seasonal flow under future climate scenarios for RCP8.5 is stronger than the RCP4.5 scenarios. Thus, climate change is expected to affect the amount and ecological quality of the streamflow, the resilience of riverine species, and the resilience of riverine species.

In general, the effects of climate change on the hydrological cycle are substantial since water is essential to both the natural world and the socioeconomic system. Climate change can cause changes in water resource availability patterns and hydrological extreme events such as floods and droughts, which can have a number of indirect effects on agriculture, food and energy production, and general water infrastructure (IPCC 2007; Kang et al. 2009). Because of the conflicting economic, political, and social interests of

riparian countries, the climate change impact will be greater in transboundary rivers like the Baro–Akobo River where water is in high demand. This is particularly true when upstream countries can have a significant impact on downstream countries (IPCC 2007; Hulme et al. 2005).

The outcomes of the climate projection study illustrate the implications of decreased water availability and its effects on agricultural output. As a result, this study suggests water harvesting strategies that could maintain water availability for agriculture and other ecosystem services to counteract future climate change impacts. The productivity of the large hydropower systems planned for the region as well as the rising demand for agricultural and transportation expansion could potentially be impacted from a water management perspective by the overall reduction in river flows and their increased variability. Therefore, the implementation of water resources development work such as hydraulic structures, which are related to irrigation and hydropower, should take into account the anticipated change in the climate. Additionally, it is necessary to implement Ethiopian Green Economy Climate-Resilience strategies to halt trends in deforestation and land degradation in order to mitigate any potential shortage of stream flow, which has been a challenge for the water supply, irrigation, and hydropower development in the basin.

Model uncertainties

The impact of climate change studies on hydrology by applying hydrological models involves various uncertainties (Fowler et al. 2007; Abdo et al. 2009). In climate change studies, the choice of GCM and RCM is the greatest source of uncertainty (Kundzewicz et al. 2018).

The discrepancy among the GCM models and regional climate change studies is manifested as a large source of uncertainty. Moreover, the climate models disagree on the magnitude and even the direction of change of climate variables in different parts of the world, particularly when it comes to rainfall (Zhang et al. 2014). In addition, the source of hydrological model uncertainty can be associated with model structure, parameter uncertainty, and data scarcity for calibration and validation processes as well as data inputs (e.g., lack of relevant spatial and temporal variability of data on climate, soils, and land uses) (Kundzewicz et al. 2018).

Despite these potential sources of uncertainties, this study made efforts to reduce uncertainties stemming from climate change, hydrological modeling, and other input data such as weather data and land use. One possibility of accounting for some of the uncertainties is using an ensemble of climate models (Teutschbein and Seibert 2010). As a result, an ensemble of multi-GCM-driven RCM simulations was used based on the different magnitudes and directions of future climate change. The most plausible emission scenarios with robust bias correction techniques are used for

the assessments of the RCMs to reduce uncertainty. The SWAT model was calibrated and validated for stream-flow data before being applied for climate change impact assessment. In addition, before running the SWAT model, this study looked for the best available data such as a high-resolution soil map (250 m), land use map (30 m), DEM (30 m), weather data quality, and all missing data were filled in to reduce uncertainties in the model projection and try to understand the impact of climate change on the hydrological process in the basin. The performance of the model showed good performance when evaluated in terms of the p -factor and the r -factor model uncertainty metrics.

Conclusions

This study assessed the expected future changes in rainfall and temperature for the Baro–Akobo River basin under the RCP4.5 (the middle situation) and RCP8.5 (business-as-usual development pathways) scenarios using different bias-corrected regional climate models from the CORDEX-Africa project. The calibrated SWAT model and the IHA software were used for a future prediction of the hydrological processes in the basin. There is less agreement between the RCMs as to the magnitude, and even direction and monthly changes in rainfall, but comparatively better agreement in temperature was predicted. In the ensemble, both maximum and minimum temperatures are projected to increase throughout the year. However, it is also shown that the increases in temperature are greater in the 2080s than in the 2030s and for minimum temperatures than maximum temperatures. In contrast, annual rainfall is projected to decrease throughout the year, but the decrease is greater in the 2080s under the RCP8.5 scenarios.

The impact of climate change scenarios on hydrology shows that the monthly and seasonal variations in stream flow will be greater when compared to the annual variation. The mean basin water balance has also resulted in a considerable decline in surface runoff, total water yield, and aquifer recharge, but the evapotranspiration projection is increasing. The hydrological flow indicators related to monthly flows indicate a decrease in the high and middle range of variability categories, while the low category shows an increasing trend. As a result, the decrease in rainfall and the increase in maximum and minimum temperatures because of climate change may impact the soil water balance by increasing both plant transpiration and soil evaporation, which will have a negative impact on crop growth and agricultural productivity. Therefore, consideration should be given to irrigation infrastructure design. Furthermore, a water storage structure is required to offset the decrease in rainfall.

In general, this study indicated the likely impacts of the predicted warmer conditions and a decrease in seasonal

water availability in the study region. This could jeopardize the water supply for irrigation, agriculture, and hydropower in the lower reaches of the catchment unless proper water management and water-saving structures are implemented. Therefore, the finding will be important for water resource policymakers to develop appropriate water management strategies and adaptation options to offset the adverse impacts of future climate change.

Declarations

Conflict of interest The authors declare no conflict of interest.

References

- Abbaspour KC, Yang J, Maximov I et al (2007) Modeling hydrology and water quality in the pre-alpine/alpine Thur watershed using SWAT. *J Hydrol* 333(2–4):413–430. <https://doi.org/10.1016/j.jhydrol.2006.09.014>
- Abbaspour KC, Rouholahnejad E, Vaghefi S et al (2015) A continental-scale hydrology and water quality model for Europe: calibration and uncertainty of a high-resolution large-scale SWAT model. *J Hydrol* 524:733–752. <https://doi.org/10.1016/j.jhydrol.2015.03.027>
- Abdo KS, Fiseha BM, Rientjes THM et al (2009) Assessment of climate change impacts on the hydrology of Gilgel Abay catchment in Lake Tana basin. *Ethiopia* 3669:3661–3669. <https://doi.org/10.1002/hyp>
- Alemayehu T, Kebede S, Liu L (2016) Nedaw D (2016) groundwater recharge under changing landuses and climate variability : the case of Baro-Akobo River Basin. *Ethiopia* 6(1):78–95
- Baldauf M, Seifert A, Förstner J, Majewski D, Raschendorfer M, Reinhardt T (2011) Operational convective-scale numerical weather prediction with the COSMO model: description and sensitivities. *Mon Wea Rev* 139:3887–3905. <https://doi.org/10.1175/MWR-D-10-05013.1>
- Bartier PM, Keller CP (1996) Multivariate interpolation to incorporate thematic surface data using inverse distance weighting (IDW). *Comput Geosci* 22:795–799. [https://doi.org/10.1016/0098-3004\(96\)00021-0](https://doi.org/10.1016/0098-3004(96)00021-0)
- Bayabil HK, Dile YT (2020) Improving hydrologic simulations of a small watershed through soil data integration. *Water (switzerland)* 12. <https://doi.org/10.3390/w12102763>
- Beyene T, Lettenmaier DP, Kabat P (2010) Hydrologic impacts of climate change on the Nile River Basin : implications of the 2007 IPCC scenarios, pp 433–461. <https://doi.org/10.1007/s10584-009-9693-0>
- Bhattacharya T, Khare D, Arora M (2020) Evaluation of reanalysis and global meteorological products in Beas river basin of North-Western Himalaya. *Environ Syst Res* 9:1–29. <https://doi.org/10.1186/s40068-020-00186-1>
- Block PJ, Souza Filho FA, Sun L, Kwon HH (2009) A streamflow forecasting framework using multiple climate and hydrological models. *J Am Water Resour Assoc* 45:828–843. <https://doi.org/10.1111/j.1752-1688.2009.00327.x>
- Bolch T, Kulkarni A, Kääb A, Huggel C, Paul F, Cogley JG, Bajracharya S (2012) The state and fate of Himalayan glaciers. *Science* 336(6079):310–314
- Christensen JH, Boberg F, Christensen OB, Lucas-Picher P (2008) On the need for bias correction of regional climate change projections of temperature and precipitation. *Geophys Res Lett* 35. <https://doi.org/10.1029/2008GL035694>
- Conway D, Schipper ELF (2011) Adaptation to climate change in Africa: Challenges and opportunities identified from Ethiopia. *Glob Environ Chang* 21:227–237. <https://doi.org/10.1016/j.gloenvcha.2010.07.013>
- Cramér H (1999) *Mathematical methods of statistics*, 9th edn. Princeton University Press, US
- Déqué M, Rowell DP, Lüthi D, Giorgi F et al (2007) An intercomparison of regional climate simulations for Europe: assessing uncertainties in model projections. *Clim Change* 81:53–70. <https://doi.org/10.1007/s10584-006-9228-x>
- Dibaba WT, Demissie TA, Miegel K (2020) Watershed hydrological response to combined land use/land cover and climate change in highland ethiopia: finchaa catchment. *Water (switzerland)* 12. <https://doi.org/10.3390/w12061801>
- Dibaba WT, Miegel K, Demissie TA (2019) Evaluation of the CORDEX regional climate models performance in simulating climate conditions of two catchments in Upper Blue Nile Basin. *Dyn Atmos Ocean* 87:101104. <https://doi.org/10.1016/j.dynatmoce.2019.101104>
- Dile YT, Berndtsson R, Setegn SG (2013) Hydrological response to climate change for Gilgel Abay River, in the Lake Tana Basin—Upper Blue Nile Basin of Ethiopia. 8:12–17. <https://doi.org/10.1371/journal.pone.0079296>
- Dile YT, Srinivasan R (2014) Evaluation of CFSR climate data for hydrologic prediction in data-scarce watersheds : an application in the Blue Nile River Basin 1:50. <https://doi.org/10.1111/jawr.12182>
- Elshamy ME, Seierstad IA, Sorteberg A (2009) Impacts of climate change on Blue Nile flows using bias-corrected GCM scenarios, pp 551–565
- Fenta AA, Yasuda H, Shimizu K, Ibaraki Y, Haregeweyn N, Kawai T, Belay AS, Sultan D, Ebabu K (2018) Evaluation of satellite rainfall estimates over the Lake Tana basin at the source region of the Blue Nile River. *Atmos Res* 212:43–53. <https://doi.org/10.1016/j.atmosres.2018.05.009>
- Fentaw F, Hailu D, Nigussie A, Melesse AM (2018) Climate change impact on the hydrology of Tekeze Basin, Ethiopia: projection of rainfall-runoff for future water resources planning. *Water Conserv Sci Eng* 3:267–278. <https://doi.org/10.1007/s41101-018-0057-3>
- Fowler HJ, Ekström M, Blenkinsop S, Smith AP (2007) Estimating change in extreme European precipitation using a multimodel ensemble. *J Geophys Res Atmos* 112. <https://doi.org/10.1029/2007JD008619>
- Fowler HJ, Kilsby CG (2007) Using regional climate model data to simulate historical and future river flows in northwest England. *Clim Change* 80:337–367. <https://doi.org/10.1007/s10584-006-9117-3>
- Fuka DR, Walter MT, Macalister C et al (2013). Using the climate forecast system reanalysis as weather input data for watershed models. <https://doi.org/10.1002/hyp.10073>
- Getachew F, Bayabil HK, Hoogenboom G, Teshome FT, Zewdu E (2021) Irrigation and shifting planting date as climate change adaptation strategies for sorghum. *Agric Water Manag* 255:106988. <https://doi.org/10.1016/j.agwat.2021.106988>
- Giorgi F (2006) Regional climate modeling: status and perspectives. *J Phys IV JP* 139:101–118. <https://doi.org/10.1051/jp4:2006139008>
- Gudmundsson L, Bremnes JB, Haugen JE, Engen-Skaugen T (2012) Technical Note: downscaling RCM precipitation to the station scale using statistical transformations – A comparison of methods. *Hydrol Earth Syst Sci* 16:3383–3390. <https://doi.org/10.5194/hess-16-3383-2012>
- Hawkins E, Sutton R (2011) The potential to narrow uncertainty in projections of regional precipitation change. *Clim Dyn* 37:407–418. <https://doi.org/10.1007/s00382-010-0810-6>
- Hengl T, Heuvelink GBM, Kempen B et al (2015) Mapping soil properties of Africa at 250 m resolution: random forests significantly

- improve current predictions. *PLoS ONE* 10:1–26. <https://doi.org/10.1371/journal.pone.0125814>
- Hoegh-Goldberg O, Bruno JF (2010). The impact of climate change on the World's Marine Ecosystems. <https://doi.org/10.1126/science.1189930>
- Houghton JT, Ding Y, Griggs DJ, et al (2001) Climate change 2001: the scientific basis. Contribution of working group I to the third assessment report of the Intergovernmental Panel on Climate Change. Cambridge, United Kingdom, and New York, NY: Cambridge University Press
- Hulme M, Doherty R, Ngara T, New M, Lister D (2001) African climate change: 1900–2100. *Climate Res* 17:145–168. <https://doi.org/10.3354/cr017145>
- Hulme M, Doherty R, Ngara T, New MG, Low PS (Ed) (2005). Global warming and African climate change: a reassessment. *Clim Change Africa*, pp 29–40. <https://doi.org/10.1017/CBO9780511535864>
- IPCC (2001) Climate change 2001: the scientific basis. The third assessment report of the intergovernmental panel on climate change. Cambridge University Press, New York
- IPCC (2007) Climate change 2007: The physical science basis. Contribution of working group I to the fourth assessment report of the intergovernmental panel on climate change. Cambridge University Press, Cambridge, UK, New York, US
- IPCC (2013) Climate change 2013: The physical science basis. In: Working Group I contribution to the fifth assessment report of the intergovernmental panel on climate change.
- IPCC (2014) Climate change 2014: Impacts, adaptation, and vulnerability. part a: global and sectoral aspects. In: Contribution of working group II to the fifth assessment report of the intergovernmental panel on climate change [Field CB, Barros VR, Dokken DJ]
- Jacob D, Barring L, Christensen OB, Christensen JH, de Castro M, Déqué M, Giorgi F, Hagemann S, Hirschi M, Jones R, Kjellström E, Lenderink G, Rockel B, Sánchez E, Schär C, Seneviratne SI, Somot S, van Ulden A, van den Hurk B (2012) An inter-comparison of regional climate models for Europe: model performance in present-day climate. *Clim Change* 81:31–52. <https://doi.org/10.1007/s10584-006-9213-4>
- Kang Y, Khan S, Ma X (2009) Climate change impacts on crop yield, crop water productivity and food security—a review. *Prog Nat Sci* 19:1665–1674. <https://doi.org/10.1016/j.pnsc.2009.08.001>
- Kiesel J, Gericke A, Rathjens H et al (2019) Climate change impacts on ecologically relevant hydrological indicators in three catchments in three European ecoregions. *Ecol Eng* 127:404–416. <https://doi.org/10.1016/j.ecoleng.2018.12.019>
- Kiprotich P, Wei X, Zhang Z et al (2021) Assessing the impact of land use and climate change on surface runoff response using gridded observations and swat+. *Hydrology* 8. <https://doi.org/10.3390/hydrology8010048>
- Koch FJ, Van Griensven A, Uhlenbrook S, et al (2012) The effects of land use change on hydrological responses in the Choke Mountain Range (Ethiopia)—a new approach addressing land use dynamics in the model SWAT. *iEMSs 2012—Manag Resour a Ltd Planet Proc 6th Bienn Meet Int Environ Model Softw Soc* 3022–3029
- Kundzewicz ZW, Krysanova V, Benestad RE et al (2018) Uncertainty in climate change impacts on water resources. *Environ Sci Policy* 79:1–8. <https://doi.org/10.1016/j.envsci.2017.10.008>
- Liu X, Liu W, Tang Q et al (2022) Global agricultural water scarcity assessment incorporating blue and green water availability under future climate change Earth's future. <https://doi.org/10.1029/2021EF002567>
- López-Ballesteros A, Senent-Aparicio J, Martínez C, Pérez-Sánchez J (2020) Assessment of future hydrologic alteration due to climate change in the Arachthos River basin (NW Greece). *Sci Total Environ* 733:139299. <https://doi.org/10.1016/j.scitotenv.2020.139299>
- McCarthy JJ, Canziani OF, Leary NA, Dokken DJ, White KS (2001) Climate change 2001: Impacts, Adaptation, and Vulnerability Contribution of Working Group II to the Third Assessment Report of the Intergovernmental Panel on Climate Change.
- Mengistu DT, Sorteberg A (2012) Sensitivity of SWAT simulated streamflow to climatic changes within the Eastern Nile River basin. 391–407. <https://doi.org/10.5194/hess-16-391-2012>
- Mengistu AG, Woldesenbet TA, Dile YT (2021a) Evaluation of the performance of bias-corrected CORDEX regional climate models in reproducing Baro-Akobo basin climate. *Theor Appl Climatol* 144:751–767. <https://doi.org/10.1007/s00704-021-03552-w>
- Mengistu AG, Woldesenbet TA, Taddele YD (2021b) Evaluation of observed and satellite-based climate products for hydrological simulation in data-scarce Baro-Akobo River Basin, Ethiopia. *Ecohydrol Hydrobiol*. <https://doi.org/10.1016/j.ecohyd.2021.11.006>
- Moriasi DN, Arnold J, Van Liew M, Bingner RL, Harmel RD, Veith TL (2007) Model evaluation guidelines for systematic quantification of accuracy in watershed simulations. *Trans Am Soc Agric Eng (ASAE)* 50:885–900
- Moss RH, Edmonds JA, Hibbard KA et al (2010) The next generation of scenarios for climate change research and assessment. *Nature* 463:747–756. <https://doi.org/10.1038/nature08823>
- Muleta TN (2021) Climate change scenario analysis for Baro-Akobo river basin. *Southwestern Ethiopia Environ Syst Res* 10. <https://doi.org/10.1186/s40068-021-00225-5>
- Munawar S, Rahman G, Farhan M, et al (2022) Future Climate Projections Using SDSM and LARS-WG Downscaling Methods for CMIP5 GCMs over the Transboundary Jhelum River Basin of the Himalayas Region
- Neitsch SL, Arnold JG, Kiniry JR, Williams JR (2011) Soil and water assessment tool theoretical documentation version 2009. Texas Water Resources Institute. <https://hdl.handle.net/1969.1/128050>
- Nikulin G, Jones C, Giorgi F et al (2012) Precipitation climatology in an ensemble of CORDEX-Africa regional climate simulations. *J Clim* 25:6057–6078. <https://doi.org/10.1175/JCLI-D-11-00375.1>
- NAPA (2007) Preparation of National Adaptation Programme of Action (NAPA) of Ethiopia. Addis Abeba
- Piani C, Haerter JO, Coppola E (2010) Statistical bias correction for daily precipitation in regional climate models over Europe. *Theor Appl Climatol* 99:187–192. <https://doi.org/10.1007/s00704-009-0134-9>
- Prentice IC, Farquhar G, Fasham M, et al (2001) The carbon cycle and atmospheric carbon dioxide. In *Climate Change 2001: The Scientific Basis* Clim; Cambridge University Press: Cambridge, UK; New York, NY, USA.
- Rathjens H, Bieger K, Srinivasan R, Arnold JG (2016) CMhyd User Manual Documentation for preparing simulated climate change data for hydrologic impact studies. p.16p
- Richter BD, Baumgartner JV, Jennifer P, Braun DP (1996) A method for assessing hydrologic alteration within ecosystems | Un metro para evaluar alteraciones hidrológicas dentro de ecosistemas. *Conserv Biol* 10:1163–1174
- Rockel B, Will A, Hense A (2008) The regional climate model COSMOCLM (CCLM4). *Meteorol Z* 17(4):347–348. <https://doi.org/10.1127/0941-2948/2008/0309>
- Saha S, Moorthi S, Pan HL et al (2010) The NCEP climate forecast system reanalysis. *Bull Am Meteorol Soc* 91:1015–1057. <https://doi.org/10.1175/2010BAMS3001.1>
- Samuelsson P, Gollvik S, Kupiainen M, Kourzeneva E, van de Berg W (2015) The surface processes of the Rossby Centre regional atmospheric climate model (RCA4), vol 1. SMHI, Norrköping, Sweden, pp 2358–2381
- Saxton K, Rawls W (2006) Soil water characteristic estimates by texture and organic matter for hydrologic solutions. *Soil Sci Soc Am J* 70:1569–1578

- Setegn SG, Rayner D, Melesse AM et al (2011) Impact of climate change on the hydroclimatology of Lake Tana Basin, Ethiopia. *Water Resour Res* 47:1–13
- Soliman ESA, Sayed MAA, Jeuland M (2009) Impact assessment of future climate change for the Blue Nile Basin, Using a RCM nested in a GCM. *Nile Basin Water Engin Sci Mag* 2:15–30
- Taye MT, Dyer E, Hirpa FA, Charles K (2018) Climate change impact on water resources in the Awash basin, Ethiopia. *Water (switzerland)* 10:1–16. <https://doi.org/10.3390/w10111560>
- Teutschbein C, Seibert J (2010) Regional climate models for hydrological impact studies at the catchment scale: a review of recent modeling strategies. *Geogr Compass* 4:834–860. <https://doi.org/10.1111/j.1749-8198.2010.00357.x>
- Teutschbein C, Seibert J (2012) Bias correction of regional climate model simulations for hydrological climate-change impact studies: review and evaluation of different methods. *J Hydrol* 456–457:12–29. <https://doi.org/10.1016/j.jhydrol.2012.05.052>
- Tahani MS, ElShamy M, Mohammed AA, Abbas MS (2013) The Development of the Baro-Akobo-Sobat sub basin and its Impact on Downstream Nile Basin Countries. *Nile Water Sci Eng J* 6:2
- Van Vuuren DP, Van Edmonds J, Kainuma M et al (2011) The representative concentration pathways: an overview. 5–31. <https://doi.org/10.1007/s10584-011-0148-z>
- UNESCO (2012) United Nation Education, Science and Cultural Organization "Ecological Sciences for Sustainable Development." from www.unesco.org.
- Worqlul A, Taddele YD, Ayana EK et al (2018) Impact of climate change on streamflow hydrology in headwater catchments of the upper Blue Nile Basin. *Ethiopia Water (switzerland)* 10. <https://doi.org/10.3390/w10020120>
- Woldesenbet TA (2022) Impact of land use and land cover dynamics on ecologically-relevant flows and blue-green water resources. *Ecohydrol Hydrobiol*. <https://doi.org/10.1016/j.ecohyd.2022.03.002>
- Woldesenbet TA, Elagib NA (2021) Spatial-temporal evaluation of different reference evapotranspiration methods based on the climate forecast system reanalysis data
- Woldesenbet TA, Elagib NA, Ribbe L, Heinrich J (2018) Catchment response to climate and land-use changes in the Upper Blue Nile sub-basins. *Ethiopia Sci Total Environ* 644:193–206. <https://doi.org/10.1016/j.scitotenv.2018.06.198>
- Worku G, Teferi E, Bantider A, Dile YT (2020) Statistical bias correction of regional climate model simulations for climate change projection in the Jemma sub-basin, upper Blue Nile Basin of Ethiopia. *Theor Appl Climatol* 139:1569–1588. <https://doi.org/10.1007/s00704-019-03053-x>
- Worku G, Teferi E, Bantider A, Dile YT (2021) Modelling hydrological processes under climate change scenarios in the Jemma sub-basin of upper Blue Nile Basin. *Ethiopia Clim Risk Manag* 31:100272. <https://doi.org/10.1016/j.crm.2021.100272>
- Zhang X, Xu YP, Fu G (2014) Uncertainties in SWAT extreme flow simulation under climate change. *J Hydrol* 515:205–222. <https://doi.org/10.1016/j.jhydrol.2014.04.064>
- Springer Nature or its licensor (e.g. a society or other partner) holds exclusive rights to this article under a publishing agreement with the author(s) or other rightsholder(s); author self-archiving of the accepted manuscript version of this article is solely governed by the terms of such publishing agreement and applicable law.